N88-21476

QUICK ACTUATING CLOSURE AND HANDLING SYSTEM

Johnny W. Allred, Dorsey E. White, III, Benjamin T. Updike, and
Peyton B. Gregory*

Abstract:

A quick activating closure and handling system, which utilitizes conical sections for locking, was developed to allow quick access of the combustor internal components of the 8-FT. High Temperature Tunnel at NASA's Langley Research Center. These critical components include the existing methane spraybar, a transpiration cooled nozzle and the new liquid oxygen (LOX) injection system housed within the combustor. A substantial cost savings will be realized once the mechanism is installed since it will substantially reduce the access time and increase the time available for conducting wind tunnel tests. A need exists for more frequent inspections when the wind tunnel operates at the more severe conditions generated by using LOX in the combustor. A loads anaylsis and a structural (finite element) analysis were conducted to verify that the new closure system is compatible with the existing pressure shell. In addition, strain gages were placed on the pressure vessel to verify how the pressure shell reacts to transient pressure loads. A scale model of the new closure system was built to verify the operation of the conical sections in the locking mechanism. The entire closure system is mounted on a handling cart for ease of operation and eliminates the need for the overhead manually operated crane. The end closure of the pressure vessel is designed to the ASME Boiler and Pressure Vessel Code, Section VIII, Division 2. The mechanism is mounted on a support cart that contains an air motor, gear boxes and screw jacks to drive the conical surfaces into the locked position in the pressure vessel.

Introduction:

The 8-Foot High Temperature Tunnel at NASA-Langley Research Center is a large blowdown wind tunnel which simulates the pressure and temperature environment encountered during Mach 7 flight at altitudes from 80 to 130,000 feet. Figure 1 shows the existing combustor which produces hot gas with maximum stagnation conditions of 27.6 MPa (4000 psig) pressure and 2220°K (4000°R) temperature. Figure 2 shows the existing end closure assembly with the methane piping attached. Methane is burned in air, with the products of combustion as the test medium, to simulate the temperature environment and provides approximately a 4-foot diameter uniform high temperature test core in the test section.

*NASA Langley Research Center
Hampton, Virginia

This unique research facility is presently being modified to allow research in the area of hypersonic air-breathing propulsion. Liquid oxygen will be introduced into the combustor for testing and evaluating large-size engine modules, full scale air-breathing missiles, flight-weight aerospace vehicle airframes, and engine structures.

Modifications to the existing tunnel will require a more frequent inspection of the combustor internal components. The combustor was designed for an internal pressure of 34.5 MPa (5000 psig) and was fabricated of thick wall material. Figure 3 shows the existing end closure which requires many man-hours for removal to allow inspection or replacement of internal components. Each piece, except for bolts, is presently handled using an overhead crane and special handling fixtures.

Present Method:

The present method is very time-consuming and requires considerable use of equipment and manpower to obtain access to the combustor internals. Figure 3 shows the 16 shear blocks with forty-six 4.45 cm (1-3/4 inch) diameter by 50.20 cm (19-3/4 inches) long bolts, a solid stud ring with twenty-four 4.8 cm(1-7/8 inch) diameter by 60.9 cm(24 inch) long studs, and a compression seal ring. Figure 4 shows the end view of the end closure assembly. The existing shear blocks, which are used in place of heavy flanges, are difficult to handle since they extend into the vessel and must be removed individually with the overhead crane and a special handling fixture. The existing shear blocks are numbered to facilitate proper reinstallation. The 46 bolts must be torqued each time the vessel is closed.

The solid flange ring (bolted to the end closure plug), the compression ring, and the seal ring require special handling fixtures and the overhead crane. The end closure plug is then removed from the vessel by means of an overhead crane and a special handling fixture as shown in Figure 5. These disassembly operations are completed by using special handling fixtures, overhead crane and a rigging crew. Approximately 164 man-hours are required to remove and reinstall the closure plug, plus detail planning, coordinating and integrating this activity between research personnel and the required trades. In the event of an unscheduled shutdown, an average of 2 days is required to remove the closure plug. This time loss translates into increased cost and reduced research productivity.

Therefore, the need exists to replace this end closure system with a design that is reliable and provides quick access to the combustor internals.

New Method:

The new method utilizes a system that includes a self-contained quick actuating closure and handling system which requires 2 hours to remove the end closure. These components are mounted to a handling cart which rolls on guide rails imbedded in the floor of the combustor building. The major components, shown in Figures 6 and 7, of the new method are the four shear blocks, a conical wedge ring to force the shear blocks radially into position for positive locking, a preload ramp that moves the shear blocks axially and

creates an initial preload between these blocks and the pressure vessel, a seal ring, and a modified closure plug. The locking mechanism is driven by an air motor and four screw jacks. The air motor operates four screw jacks to force the conical surfaces against the four shear blocks. Figure 7 shows the locked position of the shear blocks which provides the necessary preload to effectively transmit the internal pressure load directly to the grooves in the pressure vessel. These conical surfaces are designed to give the proper radial movement of the shear blocks, within the constraint imposed by the space available for longitudinal screwjack travel. These conical surfaces transmit the load directly from the plug to the pressure vessel. This new method provides system compactness and does not interfere with the required penetrations of the external piping and other equipment. The engagement of the shear blocks and the sealing of the fluid can be accomplished in a matter of minutes without the use of large bolts. Figure 8 shows the unlocked position.

Figure 9 gives a more detailed cross-section of the new method of sealing the internal gas that is more reliable than the flat metal seal used in the existing method. The seal selected provides a tapered backing ring that prevents extrusion of the o-ring. A finite element analysis shows that the radial deflection of the pressure vessel is extremely small because of the additional reinforcement from the torus which is located on the outside diameter of the pressure vessel near the seal. A backup seal is provided in the seal ring which is deformed by the pressure load acting on the preload ramp. This feature provides a backup to the primary seal. Analysis shows that the vessel is elongated in the axial direction, which unloads the clamping gaskets with the existing method. The shoulder machined in the seal ring restricts the radial movement of the preload ramp. This restriction causes the seal ring to deflect into the shoulder of the vessel. The thickness of the seal ring is sized to give the proper deflection to offset the elongation of the vessel and the compression of the shear blocks. Double seals are provided for safety reasons and provide the ability to monitor leakage from the primary seal. The leakage monitoring is accomplished by a pressure transducer located near the hole drilled through the vessel wall between seals. A lip is machined on the leading edge of the plug to minimize the potential for damaging the primary seal during installation.

This quick actuating system provides a minimum amount of wear on the locking grooves in the vessel since the final engagement is not made between the shear blocks and the vessel until the last few thousands of an inch of radial movement. The present method allows contact between the shear blocks and vessel locking grooves during assembly and disassembly causing severe wear.

This system also allows for proper adjustment of the shear blocks to the pressure vessel grooves by the use of the adjustable rods and the front tee guides shown in Figure 7. The adjustable rods contain a left-hand/right-hand threaded nut assembly to prevent the shear blocks from moving upstream when unlocking. The front tee guides prevent the shear blocks from moving downstream when locking and prevent cocking and binding during both locking

and unlocking operations. Shims are provided to allow proper adjustment. Another adjustment by installing shims exists between the seal ring and the preload ramp shown in Figure 9. This feature permits the proper tolerances for an effective use of the conical surfaces on the preload ramp. Lubrication of the sliding surfaces prevents self-locking of the wedge ring and the shear blocks.

A tee slot and a tee section shown in Figure 10 is used between each of the four shear blocks and the wedge ring to provide proper movement during assembly and disassembly. The tee section is used to lift the two bottom shear blocks from the grooves in the pressure vessel during disassembly. Proper clearance between these two items minimizes the power required to remove the shear blocks from the grooves in the pressure vessel. The initial movement of the wedge ring is accomplished before the initial movement of the shear blocks from the pressure vessel. It should be noted that the static friction of the mating surface are not overcome at the same time. These surfaces are forced together during the locking operation by the use of the air motor. The surface between the wedge ring and the shear blocks (Surface "A") is separated before the clearance between the tee and the shear blocks (Clearance "B") is closed during the disassembling operation. Shim locations are provided for final setup and assembly if needed. After the clearance is taken at the wedge ring, the jack forces are then transmitted through the surface at the bottom of the tee to overcome the static friction forces between the shear blocks and the pressure vessel.

Figure 11 shows a one-eighth scaled model which was constructed to demonstrate the operation of the closure system. The model includes the pressure shell with grooves, the preload ramp, the shear blocks, tee guides, and the wedge ring. This model was used in establishing the tolerances required for the components in the closure system and to demonstrate the design.

The locking mechanism is part of the pressure vessel and is designed in accordance with ASME Boiler and Pressure Vessel Code. The end closure meets the stress limits required by Section VIII, Division 2 of the Code. Figure 12 shows the load path of the forces resulting from the operating pressure in the combustor. A component of this axial force that is transmitted to the grooves in the pressure vessel also acts on the conical portion of the wedge ring. This component acts through the screw jack extensions and is transmitted through the vertical portion of the handling cart. Since the wheels of the cart are free to move as the combustor moves during a tunnel run, the reaction force is taken through the connecting plates and gussets, which are bolted to the closure plug. All stresses are within the ASME Code stress allowables.

Figure 13 shows the handling cart that is designed to maintain a center of gravity for the complete assembly that is well between the front and rear wheels of the cart. All components of the fuel and liquid oxygen mainfold systems are connected to the plug and can be easily inspected when the assembly is pulled from the combustor. The cart is leveled by using the manually operated screw jacks to insure that the spraybar of the methane fuel

system can be inserted into the combustor without interference with the inside diameter of the combustor. The entire system is pulled from the combustor at disassembly and pushed toward the combustor for reassembly by the use of a fork lift. The cart is mounted on tracks for proper alignment during the assembly and disassembly operations. Additional casters are provided to move the assembly laterally after the spraybar has cleared the end of the combustor.

The combustor outer shell and end retaining ring were instrumented with strain gages as shown in Figure 14 to determine if the combustor shell cycled with each pressure run of the tunnel. The instrumentation verified that the vessel did cycle with each pressure run.

Structural Evaluation:

A finite element computer model of the combustor end closure assembly was constructed for two main reasons. The first was to determine the peak stress in the grooved region of the end closure. This allowed a prediction of the cycle life and the degree to which a preload is required to reduce the number of load cycles. The second reason was to determine the deflection characteristics of the end closure so that the new design could account for such deflections.

Figure 15 shows the finite element model of a 2 degree circumferential portion of the cylindrical shell, two elements thick at 1 degree per element. The load consists of a 27.6 MPa (4,000 psi) internal pressure acting on the inside of the shell and on the face of the shear block. The model is constrained at the downstream face in the (z) direction allowing it to move radially. The load transfer between the shell and the shear block is also only in the (z) direction on the compression faces. The deformed shape is shown in Figure 16.

From the analysis, the peak stress, shown in Figures 17 and 18, is located at the inner corner of the first groove farthest downstream. The peak combined stress is 904.6 MPa (131.2 ksi) at 27.6 MPa (4000 psi) combustor pressure. This assumes full contact across all three faces of the grooved segments. The distribution of load across the first, second, and third grooves is 47%, 39% and 14% respectively. Since there are three combustor conditions, 4.2 MPa (600 psi), 13.8 MPa (2000 psi) and 27.6 MPa (4000 psi) a value of 13.8 MPa (2000 psi) is used to determine the cycle life. The total life is 18,000 cycles. From prior runs, 15.2% of the total life has been used. Therefore, the remaining cycle life is 15,260 cycles. The effect of the grooves not being simultaneously in contact was also considered. A .0254 mm (.001 inch) gap was assumed on the second and third grooves which is ten percent of the average deflection if the other two grooves were never in contact. The peak stress is 957.7 MPa (138.9 ksi) at 27.6 MPa (4000 psi) combustor pressure and the remaining cycle life is 11,500 cycles.

There are three operating conditions of the wedge ring closure mechanism: preload, release, and unload. The preload condition sets the closure plug in place and enables the combustor to take pressure. Under higher values of the coefficient of friction, the jacking force can be relieved and the wedge ring

will stay in place. The release condition relieves the wedge ring of the friction forces. After the wedge ring is released, the unload condition moves the shear blocks clear of the combustor grooves and enables the closure plug to be removed from the combustor. The reacting forces are shown in Figure 19. In addition to the normal and friction forces, there is the weight of the shear blocks and the hoop forces in the wedge ring. The reaction equations were solved, and the jacking forces were determined as a function of the coefficient of friction and the hoop force in the wedge ring.

Another variable considered was the angle of the preload ramp. Ramp angles of 5^{o} and 10^{o} were investigated. It was found that a substantial decrease in the preload and releasing jacking forces occurred using a 5^{o} ramp and a slight increase in the unload jacking force using a 5^{o} ramp. Therefore, a 5^{o} ramp is used to minimize the required jacking force. Figure 20 shows a plot of jacking force versus coefficient of friction for the three operating conditions. The jacking force is a per jack force using a total of four jacks. Wedge ring hoop forces of 0 and 44.5 kN (10,000 lbs) were considered, which tends to be the bounds depending on the final tolerances between the wedge ring and closure plug. In Figure 20, four pairs of lines are shown. The upper line is for a zero hoop force and the lower line is for a 44.5 kN hoop force. The plot also shows the variation between a preload ramp of 5^{o} and 10^{o}. Figure 21 is a plot of the normal forces as a function of the coefficient of friction for a 5^{o} preload ramp.

Summary:

A quick actuating closure and handling system has been designed to reduce the projected inspection cost and to increase the research facility productivity. The new closure system, which takes 2 hours to remove, allows easy access to the internal components of the combustor for inspection of the transpiration cooled nozzle, the fuel spraybar, and the liquid oxygen injection system. The structural integrity of the combustor is maintained while reducing the complex handling operations associated with assembly and disassembly of the closure components. The analysis shows that the fatigue life of the combustor is not reduced and that the new design meets the requirements of the ASME Pressure Vessel Code. The new design increases system reliability by providing an improved sealing system and eliminates the possibility of the unsafe handling of the large end closure components.

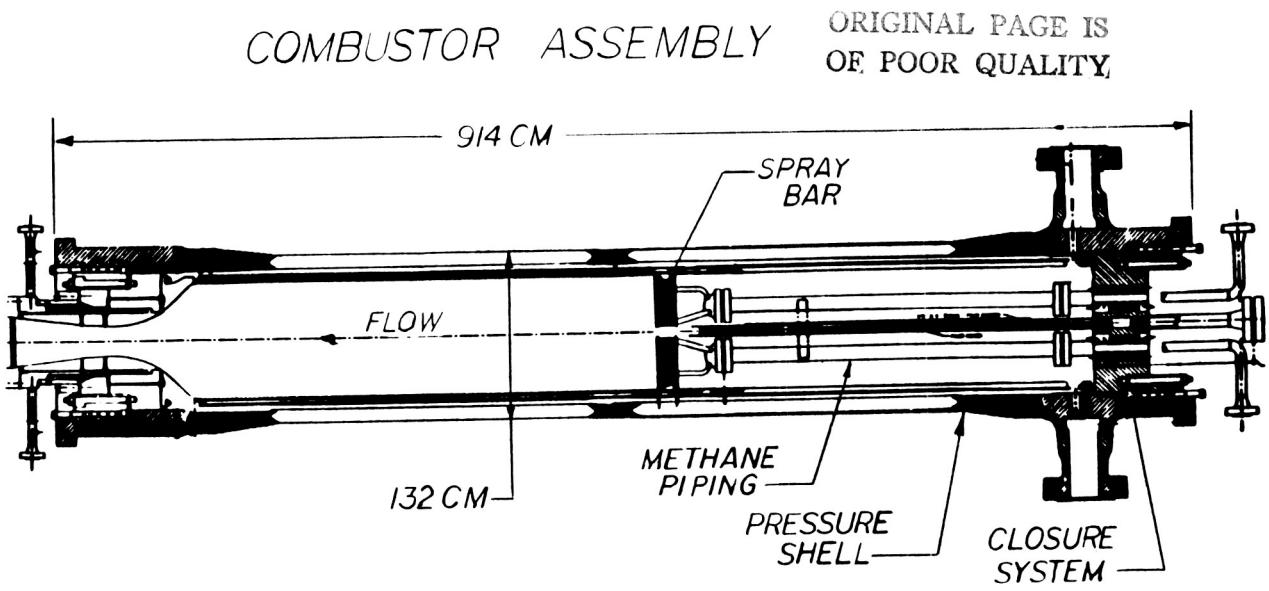

Figure 1

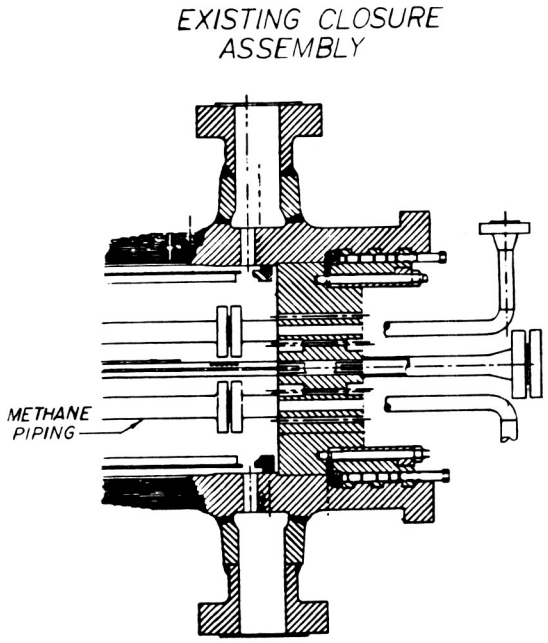

Figure 2

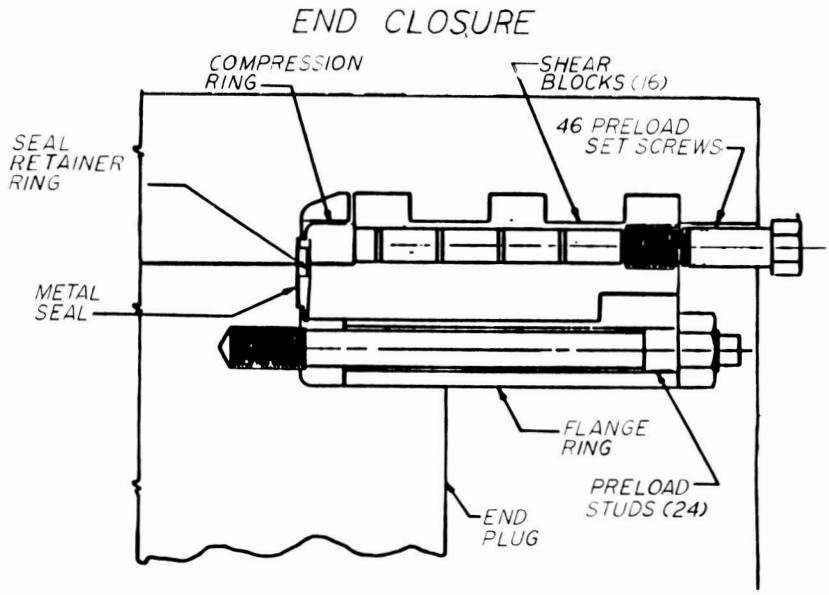

Figure 3

ORIGINAL PAGE IS
OE POOR QUALITY

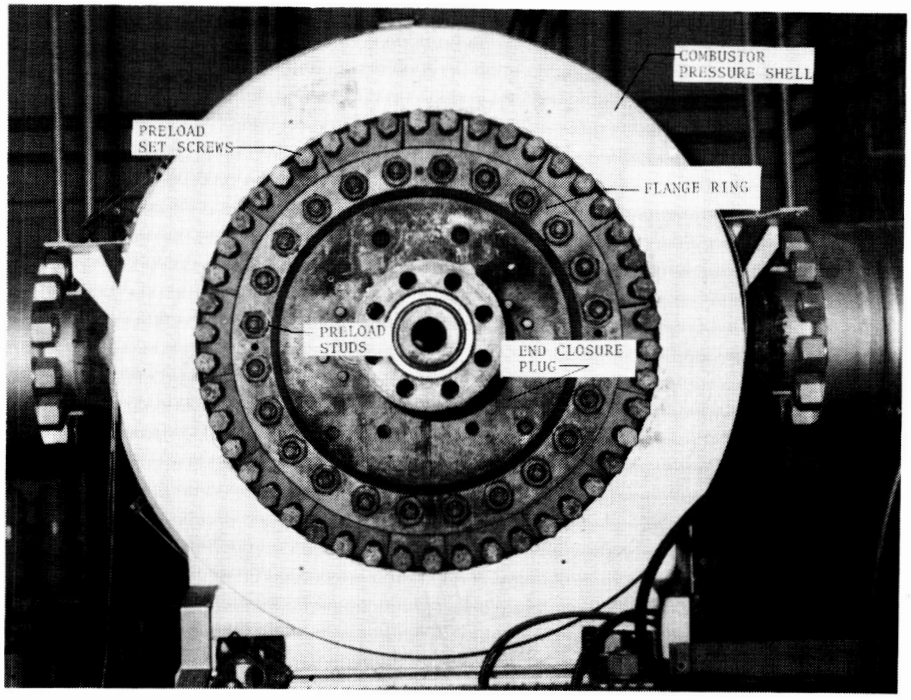

Figure 4

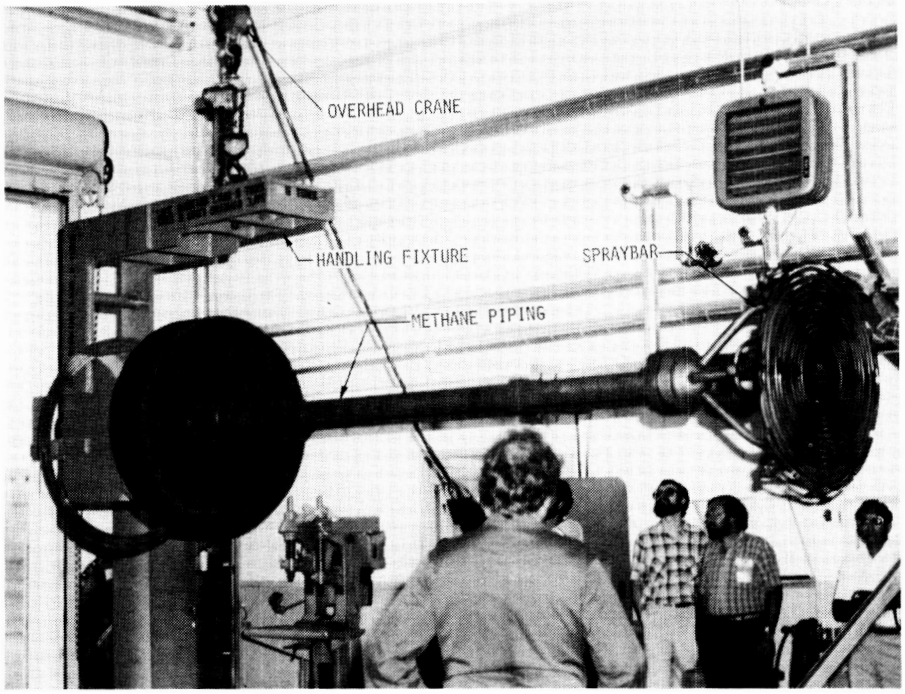

Figure 5

CLOSURE ASSEMBLY

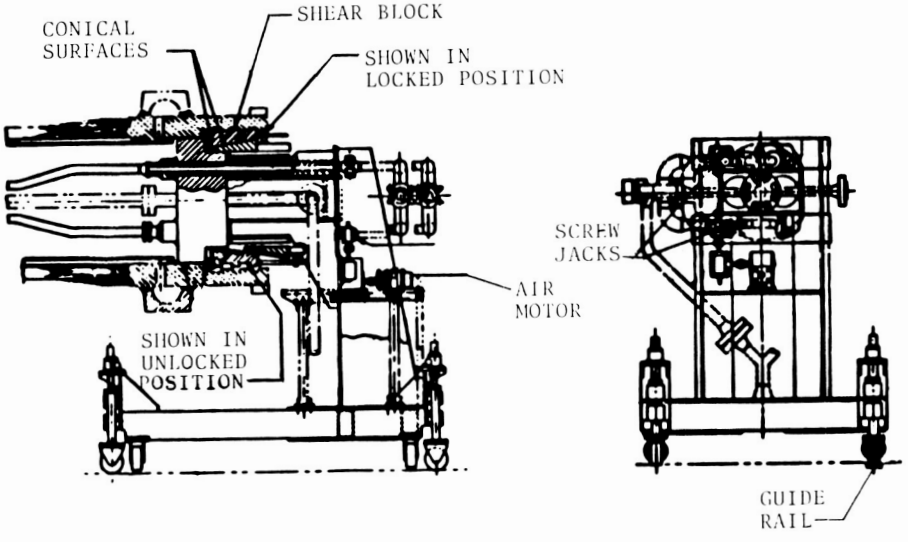

Figure 6

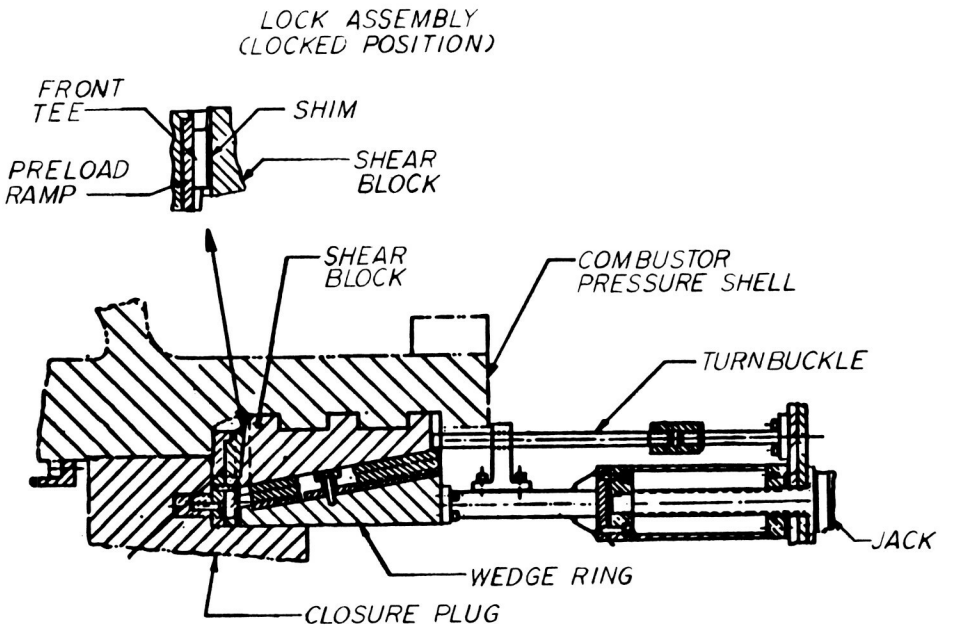

Figure 7

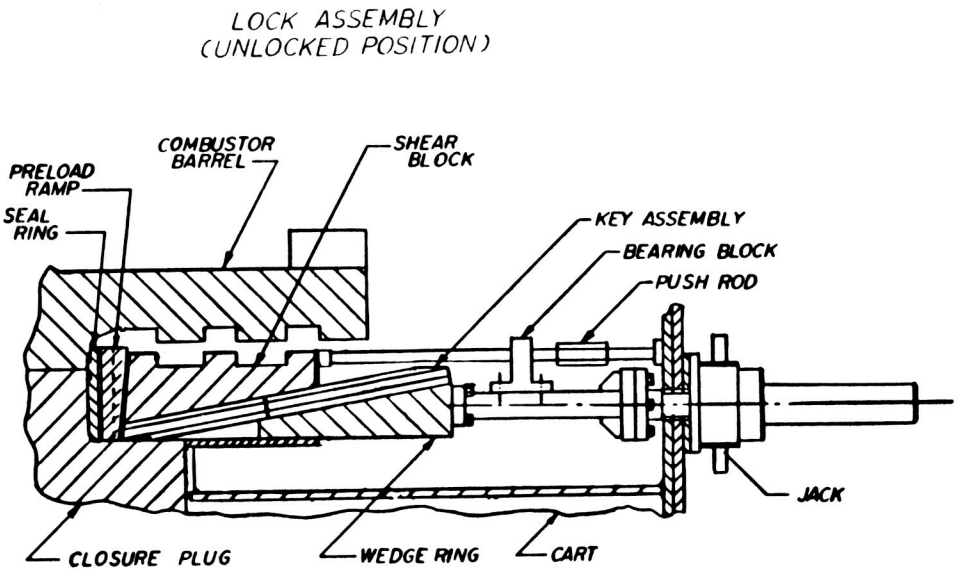

Figure 8

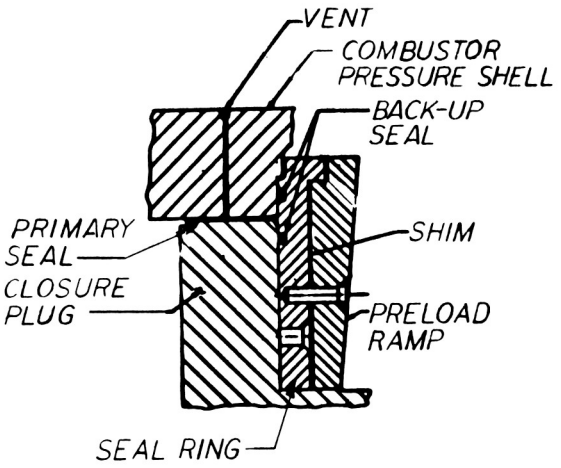

Figure 9

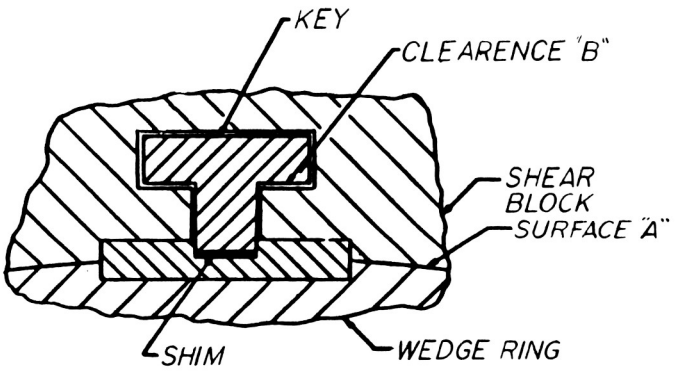

Figure 10

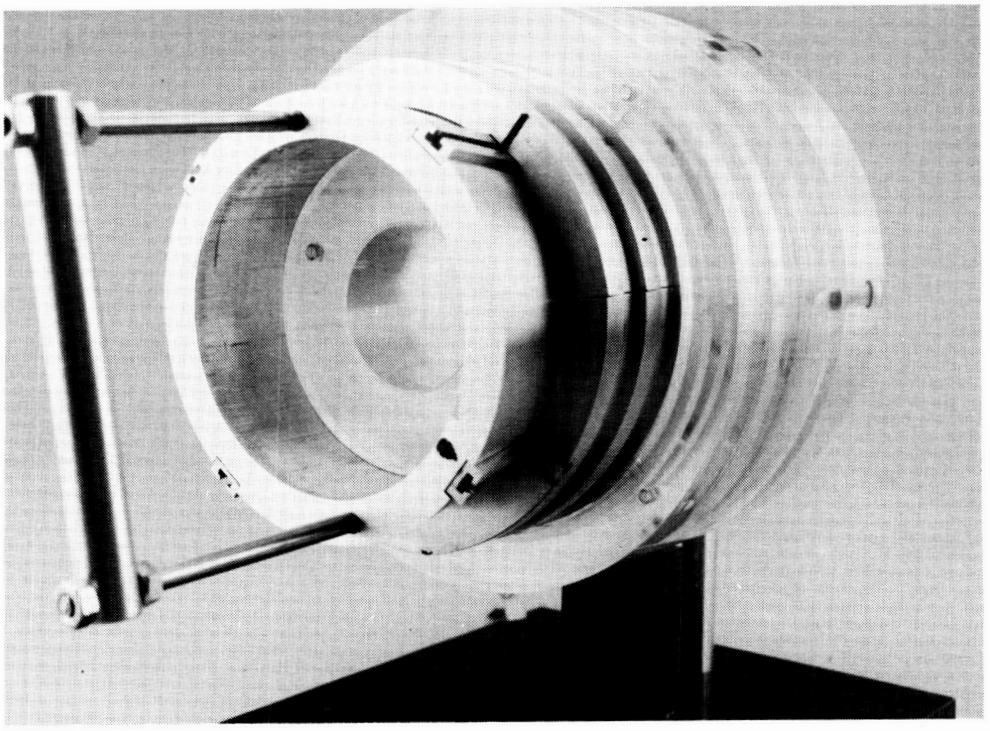

Figure 11

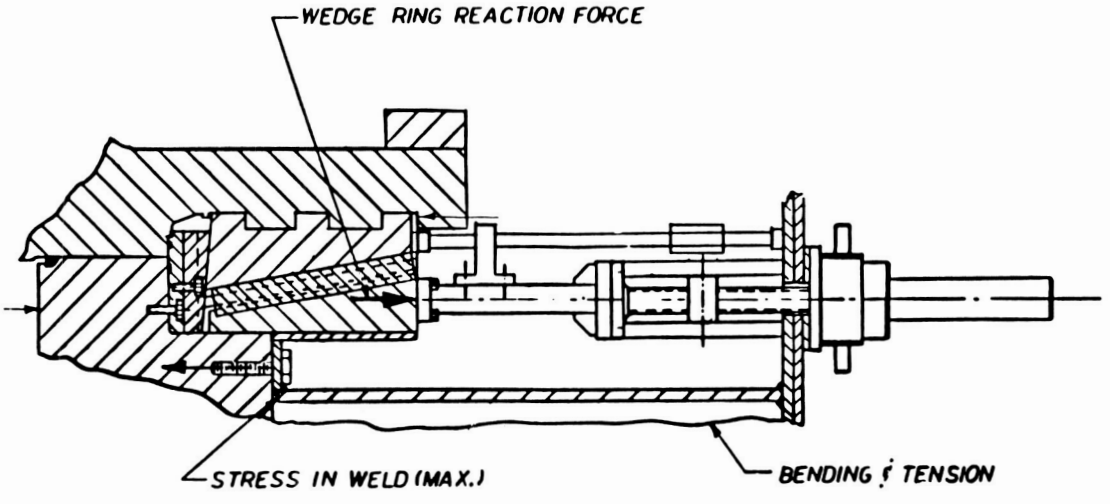

Figure 12

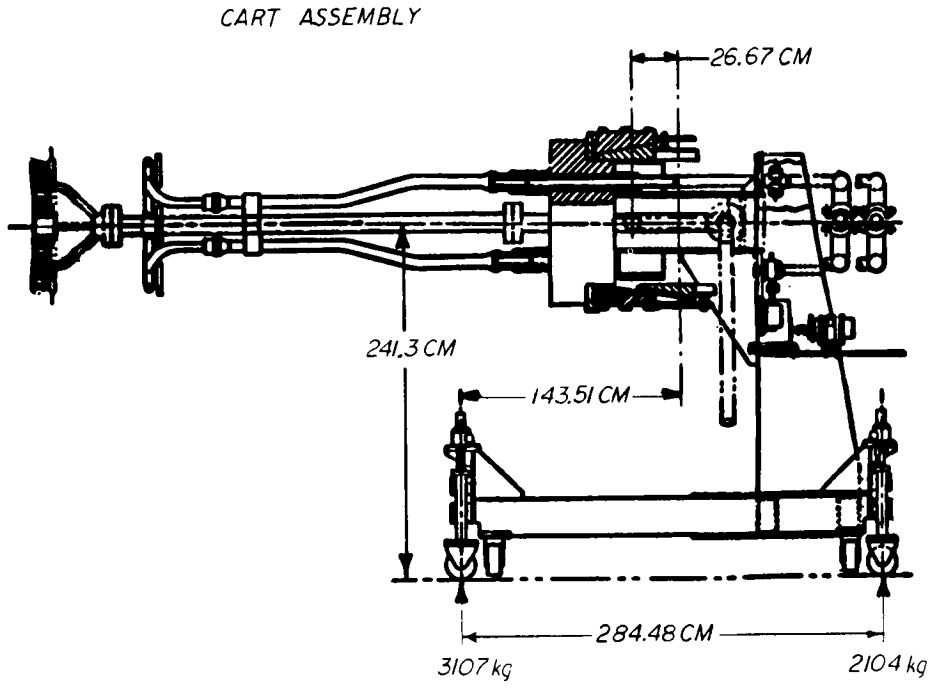

Figure 13

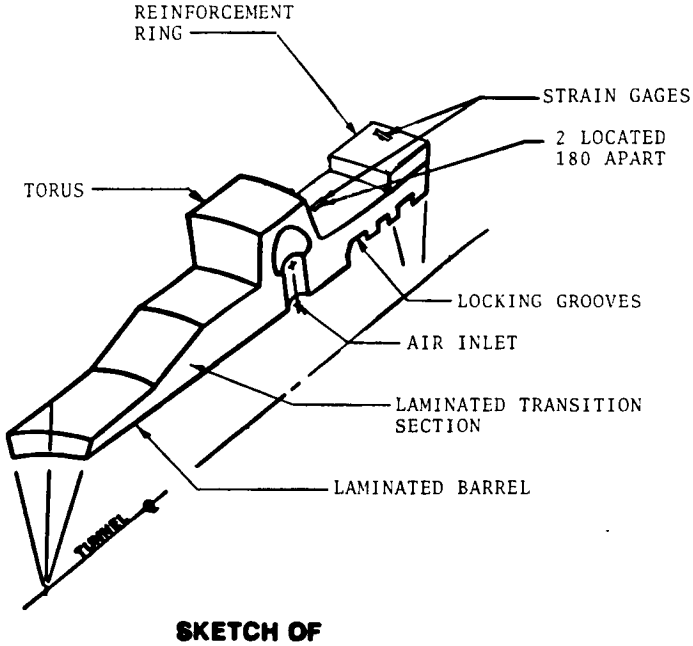

SKETCH OF FINITE ELEMENT MODEL

Figure 14

FINITE-ELEMENT MODEL

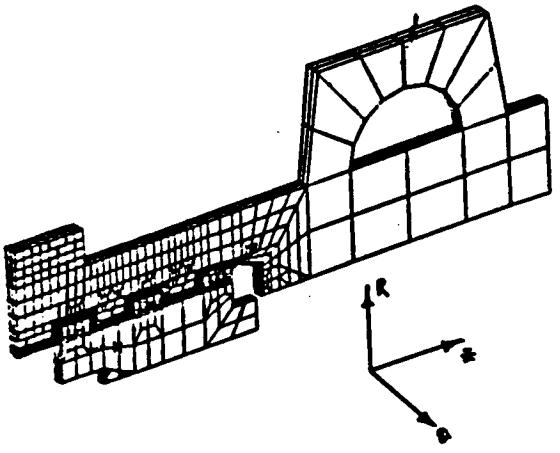

Figure 15

DEFORMED SHAPE

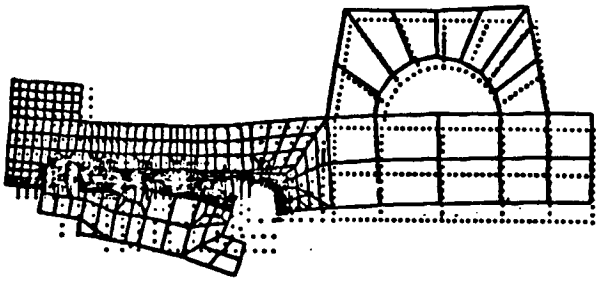

Figure 16

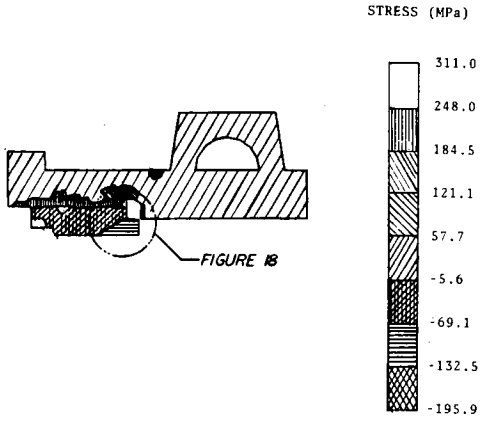

Figure 17

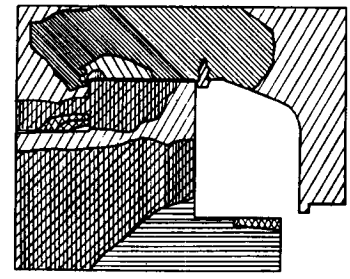

Figure 18

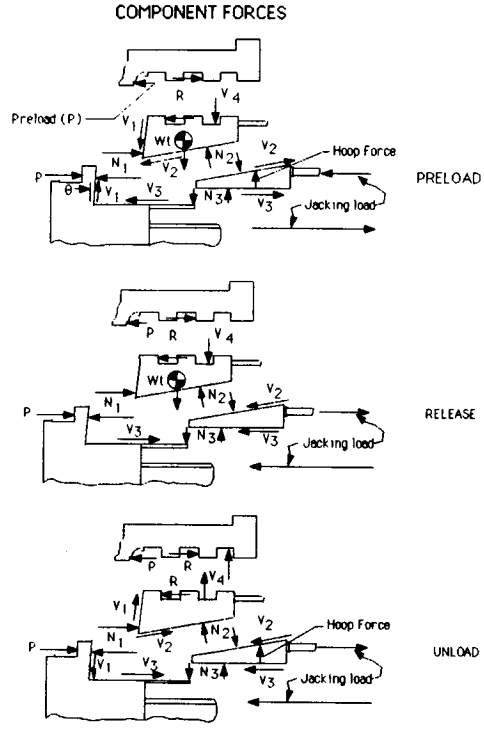

Figure 19

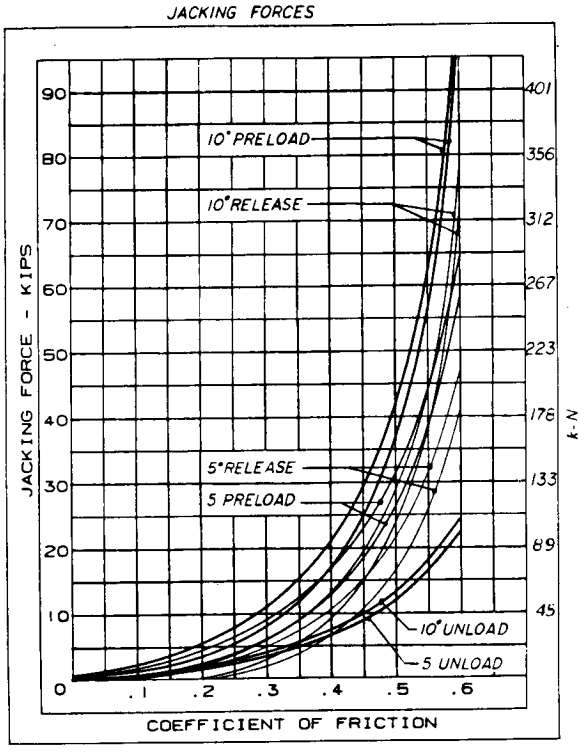

Figure 20

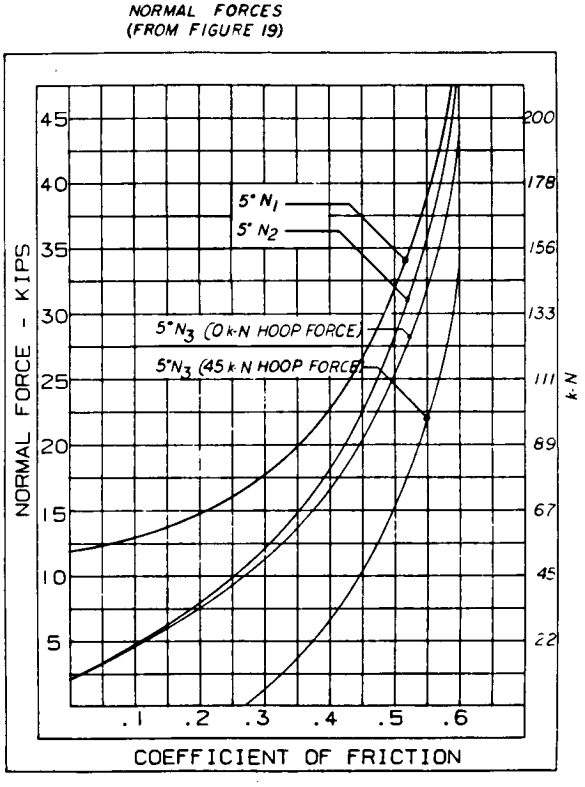

Figure 21